# Properties of one-dimensional photonic crystals containing single-negative materials

Haitao Jiang,[1] Hong Chen,[1,*] Hongqiang Li,[1] Yewen Zhang,[1] Jian Zi,[2] and Shiyao Zhu[3]
[1]*Pohl Institute of Solid State Physics, Tongji University, Shanghai, 200092, People's Republic of China*
[2]*Department of Physics, Fudan University, Shanghai 200433, People's Republic of China*
[3]*Department of Physics, Hong Kong Baptist University, Kowloon Tong, Hong Kong*
(Received 14 February 2004; published 10 June 2004)

The transmission properties of a one-dimensional photonic crystal containing two kinds of single-negative (permittivity- or permeability-negative) media are studied theoretically. We show that this structure can possess a type of photonic gap with zero effective phase ($\phi_{\mathrm{eff}}$). The zero-$\phi_{\mathrm{eff}}$ gap distinguishes itself from a Bragg gap in that it is invariant with a change of scale length and is insensitive to thickness fluctuation. In contrast to a photonic gap corresponding to zero averaged refractive index, the zero-$\phi_{\mathrm{eff}}$ gap can be made very wide by varying the ratio of the thicknesses of two media. An equivalent transmission-line model is utilized to explain the properties. A photonic quantum-well structure based on zero-$\phi_{\mathrm{eff}}$ gaps is proposed as a multiple channeled filter that is compact and robust against disorder.

DOI: 10.1103/PhysRevE.69.066607 PACS number(s): 42.70.Qs, 78.20.Ci, 41.20.Jb

## I. INTRODUCTION

Photonic crystals (PCs) have found many applications due to their unique electromagnetic properties[1]. Conventional photonic band gap (PBG) originates from the interference of Bragg scattering in a periodical dielectric structure. Since the middle frequency of the Bragg gap is inversely proportional to the lattice constant, the size of device based on the PBG is dependent on the working wavelength. For example, a microwave device based on the PBG is usually large. On the other hand, the properties of photonic materials are affected by disorder and/or fabricational tolerances. Sometimes randomness may deteriorate the PBG. In order to make devices compact and robust against disorder, some type of PBG coming from mechanisms beyond the Bragg scattering needs to be found.

One such attempt is to realize PBG in metamaterials. The metamaterials that exhibit simultaneously negative permittivity ($\varepsilon$) and permeability ($\mu$) in a frequency band are called double-negative (DNG) materials or left-handed (LH) materials [2–13]. It is demonstrated that stacking alternating layers of double-positive and DNG media leads to a type of PBG corresponding to zero (volume) averaged refractive index[9]. Such zero-$\overline{n}$ gap differs fundamentally from a Bragg gap in that it is invariant with scaling and insensitive to disorder. A number of unique transmission properties of the zero-$\overline{n}$ gap have been studied [10,11].

Besides DNG materials, the materials in which only one of the material parameters has negative value have attracted people's interest [14,15]. These single-negative (SNG) materials include the epsilon-negative (ENG) media with negative permittivity but positive permeability and the mu-negative (MNG) media with negative permeability but positive permittivity. Metamaterials with effective negative permittivity in a frequency band have been fabricated by using wire elements [16]. Metamaterials with effective negative permeability in a particular frequency range have also been obtained by utilizing split ring resonators [17]. However, people have to combine both the methods of fabricating ENG media and MNG media to form metamaterials with simultaneously negative permittivity and permeability[3,6]. Therefore, in point view of techniques, fabrication of SNG materials may be less intricate than that of DNG materials. Moreover, effective LH media can be formed by having layers of SNG media since the effective group velocity and phase velocity in such structure would be antiparallel [14]. A number of unique properties such as resonance, complete tunneling and transparency have been found in MNG-ENG bilayer structure [15].

In this paper, we find that MNG-ENG multilayer structure can possess a type of photonic gap that is distinct from a Bragg gap. When the wave impedance and *effective* phase shift in MNG layer are equal to those in ENG layer at some frequency (zero effective phase delay point), the wave can tunnel through the structure without any phase delay. Once the effective phase shift (at wave impedance matching frequency) in the MNG layer mismatches that in ENG layer, however, a gap will open at the zero effective phase (zero-$\phi_{\mathrm{eff}}$) delay point, and we call this gap the zero-$\phi_{\mathrm{eff}}$ gap. In comparison with a Bragg gap, the zero-$\phi_{\mathrm{eff}}$ gap has unique properties. Conventional Bragg gap varies with respect to a scale-length change and would be deteriorated by randomness. However, the zero-$\phi_{\mathrm{eff}}$ gap is invariant with a change of scale length and insensitive to disorder as long as the ratio of the average thicknesses of two media maintains, as we will show in Sec. II. An equivalent transmission-line (TL) model is used to explain the properties of the zero-$\phi_{\mathrm{eff}}$ gap and the connection and correspondence between the zero-$\phi_{\mathrm{eff}}$ gap and the zero-$\overline{n}$ gap are analyzed in Sec. III. In Sec. IV, a photonic quantum-well (QW) structure based on zero-$\phi_{\mathrm{eff}}$ gaps is proposed, and its properties and application as a multiple channeled filter are discussed. Finally, we conclude in Sec. V.

*Corresponding author: Email: honchenk@online.sh.cn

 

## II. INFINITE- AND FINITE-PERIODIC STRUCTURE WITH SNG MATERIALS

We suppose that

$$\varepsilon_1 = \varepsilon_a, \quad \mu_1 = \mu_a - \frac{\alpha}{\omega^2} \tag{1}$$

in MNG materials and

$$\varepsilon_2 = \varepsilon_b - \frac{\beta}{\omega^2}, \quad \mu_2 = \mu_b, \tag{2}$$

in ENG materials. It is noted these kinds of dispersion for $\mu_1$ and $\varepsilon_2$ may be realized in special microstrips [18]. In Eqs. (1) and (2), $\omega$ is the frequency measured in GHz. We consider the situation that $\mu_1$ and $\varepsilon_2$ are negative. In the following calculation, we choose $\mu_a=\varepsilon_b=1$, $\varepsilon_a=\mu_b=3$, $\alpha=\beta=100$. The thicknesses of MNG and ENG slabs are assumed to be $d_1$ and $d_2$, respectively.

First we consider an infinite-periodic structure. The dispersion relation can be obtained by using the Bloch-Floquet theorem [14]:

$$\cos\beta(d_1+d_2) = \cosh k_1d_1 \cosh k_2d_2 - \frac{1}{2}\left(\frac{\eta_1}{\eta_2}+\frac{\eta_2}{\eta_1}\right)\sinh k_1d_1 \sinh k_2d_2, \tag{3}$$

where $\beta(d_1+d_2)$ is the Bloch phase (Bloch wave vector $\beta$ times the lattice constant), the wave impedances and effective phase shifts in MNG and ENG layers are $\eta_i=\sqrt{|\mu_i/\varepsilon_i|}$, $k_i\, d_i=k\sqrt{|\varepsilon_i\mu_i|}d_i$ $(i=1,2)$, respectively; $k$ is the wave number in vacuum. Although in each layer fields are evanescent waves since the wave vectors are complex, propagation modes in the periodic structure still exist. The appearance of propagation modes can be explained with the aid of a tight-binding model in solid-state physics. When SNG layers construct a periodic structure, the localized interface modes (we will explain this unusual field behavior in detail later) in each period will interact and thus split. That is to say, the interface modes will couple each other and form propagation modes. Here in order to discuss the problem conveniently, we introduce the phase-match condition that is written as

$$k_1d_1 = k_2d_2. \tag{4}$$

The variance of band gap with different ratio of two kinds of single-negative media is shown in Fig. 1. The solid line in Fig. 1(a) corresponds to the phase-match (at wave impedance matching frequency) case and no gap exists around the zero effective phase delay point. When the phase-match condition is not satisfied, a gap opens at the zero effective phase delay point, as shown by the dashed line in Fig. 1(a). The zero-$\phi_{\text{eff}}$ gap has a unique property that distinguishes itself from a Bragg gap in that it is invariant with scaling, as shown by the dotted line in Fig. 1(a). Figure 1(b) shows the other unique feature of the zero-$\phi_{\text{eff}}$ gap. The width of the zero-$\phi_{\text{eff}}$ gap enlarges when the ratio of the thicknesses of two media increases from 2 (solid line), to 3 (dashed line) and 4 (dotted line), respectively. But the middle of each gap hardly changes. This is also quite different from a Bragg gap. Given

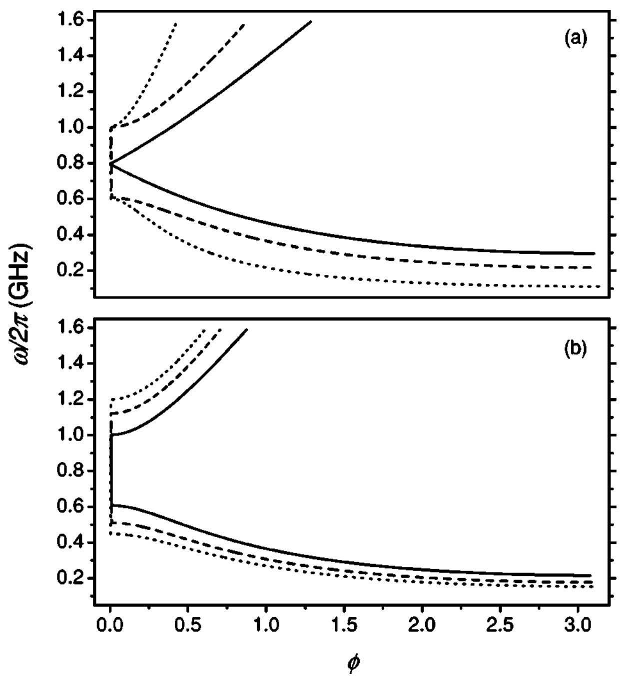


FIG. 1. The variance of band gap with different ratio of two media. (a) Solid line: $d_1=d_2=12$ mm; this corresponds to the phase match (at wave impedance matching frequency) case. Dashed line: $d_1=12$ mm, $d_2=6$ mm; a gap opens at the zero effective phase delay point. Dotted line: $d_1$ and $d_2$ are scaled by $1/2$ respectively; the gap remains invariant. (b) The gap enlarges when the ratio of the thicknesses of two media increases; $d_1=12$ mm. Solid line: $d_1/d_2=2$. Dashed line: $d_1/d_2=3$. Dotted line: $d_1/d_2=4$.

material parameters, the middle of a Bragg gap will shift noticeably while the width of the gap will change a little when the ratio of the thicknesses of the two types of layers varies. These unusual features of the zero-$\phi_{\text{eff}}$ gap can be well understood by using an equivalent transmission-line model, as demonstrated in Sec. III.

For a finite-periodic structure, the fields within each layer are a superposition of forward-decaying and backward-decaying evanescent waves. Suppose a transverse electric wave is normally (along the $z$ direction) incident on the structure. The transmission properties and field distributions of the structure can be obtained by means of a transfer matrix method. Figure 2 shows another unique feature of the zero-$\phi_{\text{eff}}$ gap. The zero-$\phi_{\text{eff}}$ gap is even robust against disorder. The solid line in Fig. 2 is the transmittance through 16 periods, the ratio of $d_1$ and $d_2$ is 2. The dotted line corresponds to the transmittance through the same media but the lattice constant is scaled by $2/3$. The dashed line is the transmittance through a structure with thickness fluctuation of ±4 mm over 32 layers on the condition that the ratio of average $d_1$ and $d_2(\overline{d_1}/\overline{d_2})$ remains 2. The independence of the zero-$\phi_{\text{eff}}$ gap on scaling means that photonic devices based on such PBG can be made very compact. It may be surprising that the zero-$\phi_{\text{eff}}$ gap is robust against disorder as long as the ratio of *average* $d_1$ and $d_2$ maintains. These properties are connected with the unusual field behavior inside MNG-ENG multilayer structure. At each interface between MNG material and ENG material, boundary condition requires that the tangential

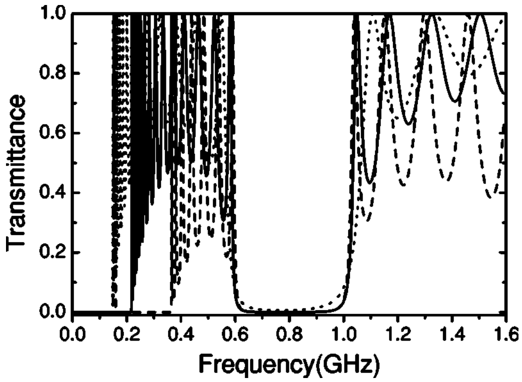


FIG. 2. Solid line: Transmittance through 16 periods, $d_1=12$ mm, $d_2=6$ mm. Dotted line: the lattice constant is scaled by 2/3. Dashed line: thickness fluctuation (random uniform deviate) of ±4 mm averaged over 32 layers (+ and − are equally probable).

component of electric and magnetic fields must be continuous. Magnetic field is proportional to the permeability multiplying the derivative of electric field. Since the permeability of MNG and ENG materials has opposite signs, the derivative of electric field must change sign when the electric field runs across the interface. As a result, the field is localized at each interface. The field distributions corresponding to the low (high) band edge frequency $\omega_L(\omega_H)$ of the zero-$\phi_{\mathrm{eff}}$ gap (the solid line in Fig. 2) are shown in Figs. 3(a) and 3(b) respectively. The field behavior is quite different from that of a Bragg gap. For the Bragg gap, the standing-wave fields corresponding to the low (high) band edge frequency are localized inside the high (low) refractive index media. So the Bragg gap depends greatly on scaling. For the zero-$\phi_{\mathrm{eff}}$ gap, the fields corresponding to the band edges are localized at each interface of two media. It is the difference of field behavior that may lead to the distinct properties of the Bragg gap and the zero-$\phi_{\mathrm{eff}}$ gap.

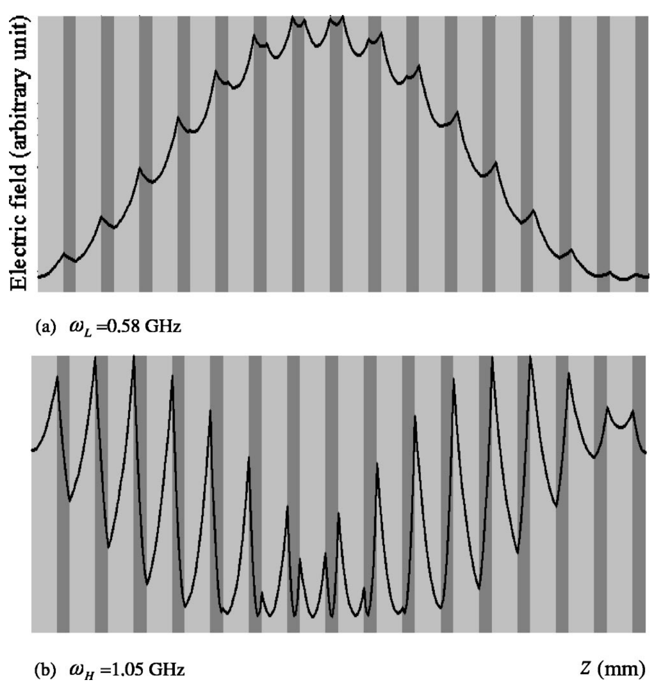


FIG. 3. The electric field distributions corresponding to the low band edge frequency $\omega_L$ (a) and high band edge frequency $\omega_H$ (b) of the solid line in Fig. 2.

## III. EQUIVALENT TRANSMISSION-LINE MODEL FOR THE MNG-ENG MULTILAYER

Since $\mu_1$ and $\varepsilon_2$ are dispersive, the mathematical expressions of the band edge frequencies deriving from Eqs. (3) are cumbersome. In order to capture the essential characteristic of the zero-$\phi_{\mathrm{eff}}$ gap, we use a method based on equivalent transmission-line (TL) models. Equivalent TL models have been utilized to analyze the properties of MNG-ENG bilayer structure [15]. In TL models, MNG material can be viewed as distributed series (left-handed) and shunt (right-handed) capacitance while ENG material can be viewed as distributed series (right-handed) and shunt (left-handed) inductance.

We suppose that $C_R^0, C_L^0(L_R^0, L_L^0)$ are the per-unit-length right-handed and left-handed capacitance (inductance). For a MNG layer with $d_1$ length, the equivalent lumped right-handed (left-handed) capacitance $C_R^m(C_L^m)$ can be written as: $C_R^m=C_R^0 d_1, C_L^m=C_L^0/d_1$; for a ENG layer with $d_2$ length, the equivalent lumped right-handed (left-handed) inductance $L_R^e(L_L^e)$ can be written as: $L_R^e=L_R^0 d_2, L_L^e=L_L^0/d_2$. For MNG-ENG periodic structure, the equivalent transmission lines can be viewed as composite right/left-handed transmission lines. For a unit cell of such transmission lines, one can obtain the dispersion relation by using the transmission matrix and Bloch-Floquet theorem [19]:

$$\cos(\beta d) = 1 - \frac{1}{2}\left[\frac{1}{\omega^2 L_L^e C_L^m} + \omega^2 L_R^e C_R^m - \left(\frac{L_R^e}{L_L^e} + \frac{C_R^m}{C_L^m}\right)\right], \tag{5}$$

where $\beta$ is Bloch wave vector, $d=d_1+d_2$. From Eqs. (5), supposing that $L_L^e C_R^m > L_R^e C_L^m$, we obtain band edge frequencies of a gap as

$$\omega_L = \frac{1}{\sqrt{L_L^e C_R^m}} = \sqrt{\frac{d_2}{d_1}}\frac{1}{\sqrt{L_L^0 C_R^0}},$$

$$\omega_H = \frac{1}{\sqrt{L_R^e C_L^m}} = \sqrt{\frac{d_1}{d_2}}\frac{1}{\sqrt{L_R^0 C_L^0}}. \tag{6}$$

The gap marked by $\omega_L$ and $\omega_H$ is equivalent to the zero-$\phi_{\mathrm{eff}}$ gap. Since $L_L^0$, $C_R^0$, $L_R^0$, $C_L^0$ are only connected with material parameters, from Eqs. (6) we can see that the band edges depend on the ratio of $d_1$ and $d_2$. The band edges therefore remain invariant when $d_1$ and $d_2$ are multiplied by a scaling factor, respectively. Moreover, with the increase of the ratio of $d_1$ and $d_2$, $\omega_H$ increases while $\omega_L$ decreases. So the gap enlarges and its middle hardly shifts.

From Eqs. (5), we can also obtain the group velocity

$$v_g = \frac{d\omega}{d\beta} = \frac{d\sin(\beta d)}{\omega L_R^e C_R^m - 1/(\omega^3 L_L^e C_L^m)}. \tag{7}$$

For $\omega<\omega_L$, $\omega L_R^e C_R^m - 1/(\omega^3 L_L^e C_L^m) < 0$, then $v_g<0$, this corresponds to the left-handed modes; for $\omega>\omega_H$, $\omega L_R^e C_R^m$

$-1/(\omega^3 L_L^e C_L^m) > 0$, then $v_g > 0$, this corresponds to the right-handed modes. Besides, we can derive the Eqs. (4) (phase-match condition) through the equivalent TL model. When the gap closes, we obtain

$$L_L^e C_R^m = L_R^e C_L^m \Leftrightarrow \frac{1}{C_L^0} C_R^0 d_1^2 = \frac{1}{L_L^0} L_R^0 d_2^2. \tag{8}$$

In equivalent TL models

$$C_R^0 = A_1 \varepsilon_1, \frac{1}{C_L^0} = \omega^2 |L_{\text{eq}}| = A_2 \omega^2 |\mu_1|,$$

$$L_R^0 = A_2 \mu_2, \frac{1}{L_L^0} = \omega^2 |C_{\text{eq}}| = A_1 \omega^2 |\varepsilon_2|, \tag{9}$$

where $A_1$ and $A_2$ are two positive constant coefficients depending on the geometry of the equivalent transmission line. Substituting Eqs. (9) into Eqs. (8), we can obtain the Eqs. (4). This confirms that the phase mismatch leads to the formation of the zero-$\phi_{\text{eff}}$ gap.

Here we discuss the connection between the zero-$\phi_{\text{eff}}$ gap and the zero-$\bar{n}$ gap. The zero-$\bar{n}$ gap and the zero-$\phi_{\text{eff}}$ gap are obtained from DPS-DNG and MNG-ENG multilayer structure, respectively. They have similarities in some ways and differences in other ways. They both lie between left-handed modes and right-handed modes, and are invariant with scaling and insensitive to disorder. However, the zero-$\phi_{\text{eff}}$ gap originates from the interaction of evanescent waves, while the zero-$\bar{n}$ gap comes from the interaction of propagating waves. Moreover, the zero-$\phi_{\text{eff}}$ gap has one unique property that the zero-$\bar{n}$ gap does not possess. The width of the zero-$\phi_{\text{eff}}$ gap with almost fixed middle can be enlarged by varying the ratio of the thicknesses of two media when material parameters are given. However, the zero-$\bar{n}$ gap opens at a frequency satisfying zero averaged refractive index condition. Given material parameters, the middle of the zero-$\bar{n}$ gap will shift noticeably to meet the zero-$\bar{n}$ condition when the ratio of the thicknesses of two media varies. At the same time, the width of the zero-$\bar{n}$ gap changes a little. This is similar to that of a Bragg gap. Therefore, the zero-$\bar{n}$ gap is usually not wide while the zero-$\phi_{\text{eff}}$ gap can be made very wide by varying the ratio of the thicknesses of two media.

## IV. PHOTONIC QUANTUM-WELL STRUCTURE BASED ON ZERO-$\phi_{\text{eff}}$ GAPS

Conventional photonic quantum-well (QW) structures are based on Bragg gaps [20]. Since photonic barriers based on Bragg gaps depend on scaling and disorder, the quantized confined photonic states in the well are strongly dependent on scaling and randomness. Even small thickness fluctuation in photonic barrier region will destroy the confined states, which limits applications of photonic QW structures such as multiple channeled filtering. However, if photonic barriers are based on zero-$\phi_{\text{eff}}$ gaps, the confined states in the well will be insensitive to scaling and disorder, as shown in Fig. 4. Suppose that a structure is made of *AB* and *CD* photonic crystals. The thicknesses of *A*, *B*, *C* and *D* are assumed to be $d_1$, $d_2$, $d_3$ and $d_4$ respectively. *CD* photonic crystal can be taken as a photonic well if the ratio of $d_1$ and $d_2$ is chosen to satisfy the phase-match (at wave impedance matching frequency) condition. And *AB* photonic crystal can be taken as a photonic barrier for another arbitrary ratio of $d_3$ and $d_4$ that does not meet the phase-match condition. The solid line in Fig. 4 is the transmittance through $(AB)_{16}$ $(CD)_8$ $(BA)_{16}$ photonic QW structure. The dotted line corresponds to the transmittance through the same media but the unit cell size is scaled by 2/3. The dashed line is the transmittance through a structure with thickness fluctuation of ±2 mm averaged over $(AB)_{16}$ and $(BA)_{16}$. The very weak dependence of the confined states on scaling and disorder will make multiple channeled filtering more practical.

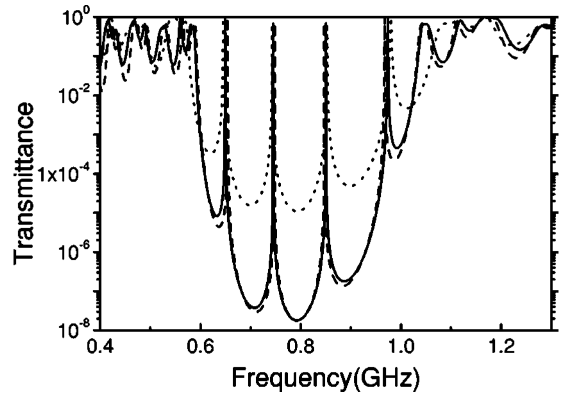


FIG. 4. Solid line: Transmittance through $(AB)_{16}(CD)_8(BA)_{16}$ photonic quantum-well structure; $d_1$=12 mm, $d_2$=6 mm, $d_3$=$d_4$=14 mm. Dotted line: the lattice constant of *AB* is scaled by 2/3. Dashed line: thickness fluctuation of ±2 mm averaged over $(AB)_{16}$ and $(BA)_{16}$.

## V. CONCLUSION

In conclusion, we showed that one-dimensional PCs containing single-negative materials can possess a type of PBG with zero effective phase. The zero-$\phi_{\text{eff}}$ gap is distinct from a Bragg gap in that it is invariant with scaling and survives under randomness. An equivalent transmission-line model is used to explain the properties. Finally, the properties of the zero-$\phi_{\text{eff}}$ gap can be utilized to construct a photonic quantum-well structure that is compact and robust against disorder.

## ACKNOWLEDGMENTS

This research was partly supported by CNKBRSF (Grant No. 2001CB610406), CNSF, Shanghai Science and Technology Committee, FRG from HKBU, and by RGC from HK Government.

[1] E. Yablonovitch, Phys. Rev. Lett. **58**, 2059 (1987); S. John, *ibid.* **58**, 2486 (1987).
[2] V. G. Veselago, Sov. Phys. Usp. **10**, 509 (1968).
[3] D. R. Smith, W. J. Padilla, D. C. Vier, S . C. Nemat-Nasser, and S. Schultz, Phys. Rev. Lett. **84**, 4184 (2000).
[4] D. R. Smith and N. Kroll, Phys. Rev. Lett. **85**, 2933 (2000).
[5] J. B. Pendry, Phys. Rev. Lett. **85**, 3966 (2000).
[6] R. A. Shelby, D. R. Smith, and S. Schultz, Science **292**, 77 (2001).
[7] Z. M. Zhang and C. J. Fu, Appl. Phys. Lett. **80**, 1097 (2002).
[8] J. Pacheco, Jr., T. M. Grzegorczyk, B.-I. Wu, Y. Zhang, and J. A. Kong, Phys. Rev. Lett. **89**, 257402 (2002).
[9] J. Li, L. Zhou, C. T. Chan, and P. Sheng, Phys. Rev. Lett. **90**, 083901 (2003).
[10] I. V. Shadrivov, A. A. Sukhorukov, and Y. S. Kivshar, Appl. Phys. Lett. **82**, 3820 (2003).
[11] H. T. Jiang, H. Chen, H. Q. Li, Y. W. Zhang, and S. Y. Zhu, Appl. Phys. Lett. **83**, 5386 (2003).
[12] L. Zhou, C. T. Chan, and P. Sheng, Phys. Rev. B **68**, 115424 (2003).
[13] A. A. Houck, J. B. Brock, and I. L. Chuang, Phys. Rev. Lett. **90**, 137401 (2003).
[14] D. R. Fredkin and A. Ron, Appl. Phys. Lett. **81**, 1753 (2002).
[15] A. Alù and N. Engheta, IEEE Trans. Antennas Propag. **51**, 2558 (2003).
[16] J. B. Pendry, A. J. Holden, W. J. Stewart, and I. Youngs, Phys. Rev. Lett. **76**, 4773 (1996).
[17] J. B. Pendry, A. J. Holden, D. J. Robbins, and W. J. Stewart, IEEE Trans. Microwave Theory Tech. **47**, 2075 (1999).
[18] G. V. Eleftheriades, A. K. Iyer, and P. C. Kremer, IEEE Trans. Microwave Theory Tech. **50**, 2702 (2002).
[19] A. Sanada, C. Caloz, and T. Itoh, IEEE Microw. Wirel. Compon. Lett. **14**, 68 (2004).
[20] F. Qiao, C. Zhang, J. Wan, and J. Zi, Appl. Phys. Lett. **77**, 3698 (2000).